Supplement of

Effects of Liquid–Liquid Phase Separation and Relative Humidity on the Heterogeneous OH Oxidation of Inorganic-Organic Aerosols: Insights from Methylglutaric Acid/Ammonium Sulfate Particles

Hoi Ki Lam[1], Rongshuang Xu[1], Jack Choczynski[2], James F. Davies[2], Dongwan Ham[3], Mijung Song[3], Andreas Zuend[4], Wentao Li[5], Ying-Lung Steve Tse[5], Man Nin Chan [1,6]

[1]Earth System Science Programme, Faculty of Science, The Chinese University of Hong Kong, Hong Kong, China

[2]Department of Chemistry, University of California Riverside, Riverside, CA, USA

[3]Department of Earth and Environmental Sciences, Jeonbuk National University, Jeollabuk-do, Republic of Korea

[4]Department of Atmospheric and Oceanic Sciences, McGill University, Montreal, Québec, Canada

[5]Departemnt of Chemistry, The Chinese University of Hong Kong, Hong Kong, China'

[6]The Institute of Environment, Energy and Sustainability, The Chinese University of Hong Kong, Hong Kong, China

Corresponding author: mnchan@cuhk.edu.hk

Table S1. Composition, viscosity, diffusion coefficient and mixing time scale of aqueous droplets containing 3-MGA and ammonium sulfate (AS) in an organic-to-inorganic dry mass ratio (OIR) = 1 at different RH predicted by the AIOMFAC-LLE.

RH (%)	**55**	**60**	**65**	**70**	**75**	**80**	**85**	**88**
Salt-rich phase (Phase α)								
Mass fraction of 3-MGA	0.00132	0.00372	0.00904	0.0202			/	/
Mass fraction of AS	0.658	0.616	0.569	0.514			/	/
Mass fraction of H_2O	0.341	0.380	0.422	0.466			/	/
Organic-rich phase (Phase β)								
Mass fraction of 3-MGA	0.612	0.596	0.574	0.546			/	/
Mass fraction of AS	0.218	0.209	0.199	0.190			/	/
Mass fraction of H_2O	0.170	0.196	0.226	0.263			/	/
Thickness of outer organic rich layer (nm)	24.9	24.6	24.2	23.6			/	/
Well-mixed phase								
Mass fraction of 3-MGA	/	/	/	/	0.292	0.262	0.224	0.197
Mass fraction of AS	/	/	/	/	0.292	0.262	0.224	0.197
Mass fraction of H_2O	/	/	/	/	0.417	0.476	0.552	0.606
Viscosity of the organic-rich phase (Pa s)	0.0958	0.0636	0.0421	0.0275	/	/	/	/
Diffusion coefficient of 3-MGA molecules in organic-rich phase ($\times 10^{-12}$ m^2 s^{-1})	6.15	9.26	14.0	21.4	/	/	/	/
Diffusive mixing time of organic-rich phase (μs)	10.2	6.6	4.2	2.6	/	/	/	/

Note: The particle radius was about 85.5 - 91.5 nm over the RH range.

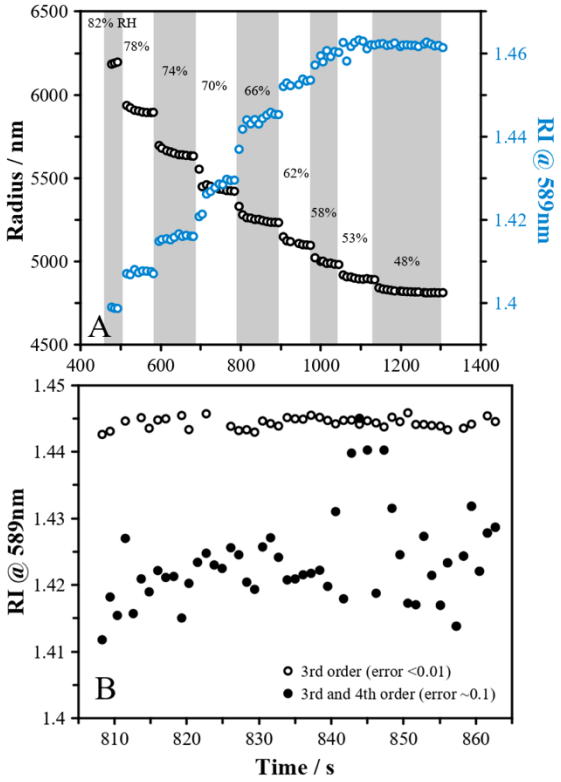

Figure S1. (A) Radius (black) and refractive index (blue) of an aqueous 3-MGA/AS droplet (OIR = 1) levitated in a LQ-EDB as a function of time upon dehumidification at room temperature using 3rd order mode. (B) The refractive index as a function of time using 3rd order mode and 4th order mode, respectively.

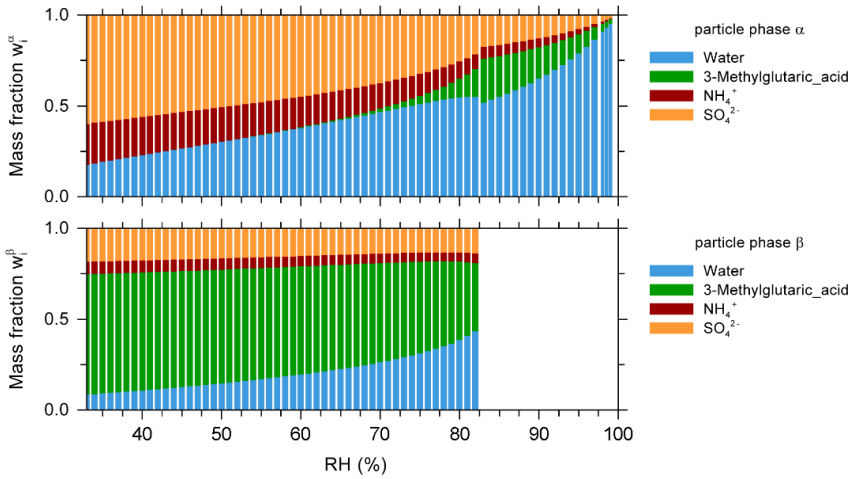

Figure S2. AIOMFAC-LLE predicted equilibrium composition of aqueous 3-MGA/AS droplets (OIR = 1) as a function of RH at T = 293 K. The upper panel shows the mass fraction of different components in the salt-rich phase (phase α). The lower panel shows the mass fraction of different components in the organic-rich phase (phase β).

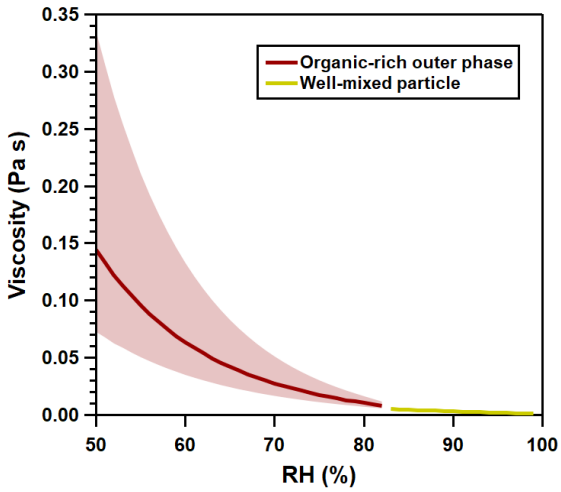

Figure S3. The viscosity estimated using AIOMFAC-VISC method of the organic-rich outer phase (phase β) of phase-separated and well-mixed 3-MGA/AS droplets (OIR = 1) as a function of RH at T = 293 K, with the shaded regions indicating the uncertainty in model estimation.

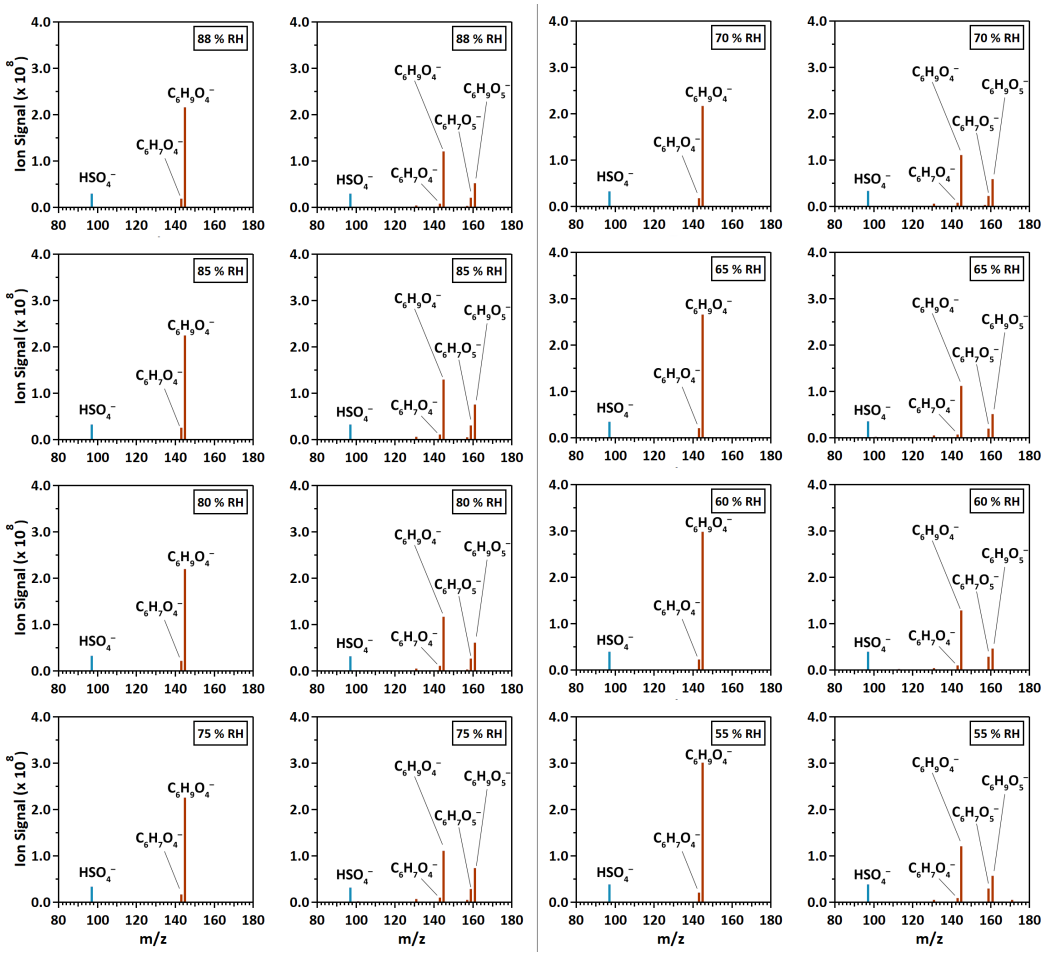

Figure S4. Aerosol-DART mass spectra of 3-MGA/AS aerosols with OIR = 1 before (left each pair of panels at the same RH) and after (right each pair of panels) heterogeneous OH oxidation at different RH. Color scheme: brown = organic species, blue = inorganic species.

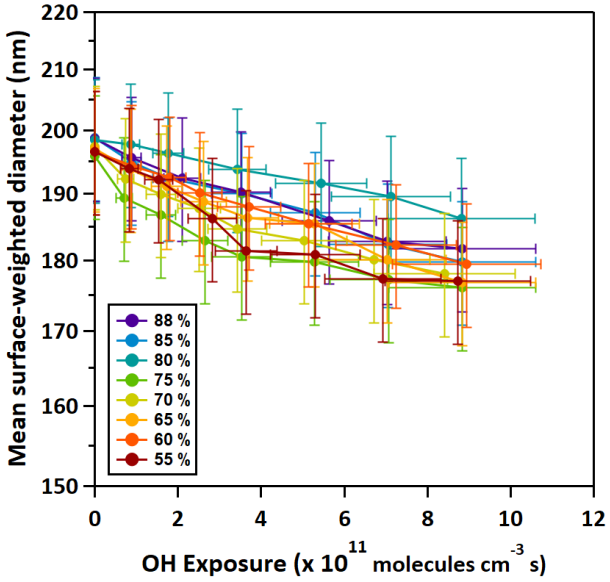

Figure S5. The change in the diameter of 3-MGA/AS aerosols (OIR = 1) upon heterogeneous OH oxidation as a function of RH and OH exposures.

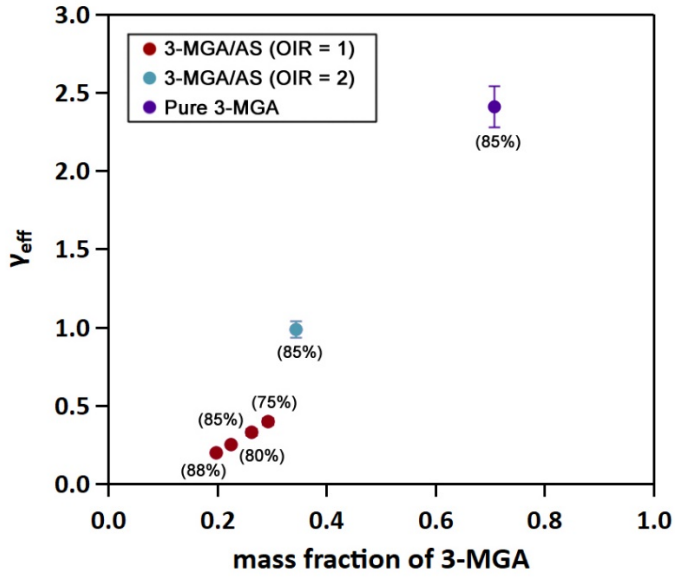

Figure S6. γ_{eff} as a function of mass fraction of pure 3-MGA aerosols at different RH and 3-MGA/AS aerosols with different OIR at 85%RH (with data of pure 3-MGA, 3-MGA/AS at OIR = 2 and 1).

Molecular Dynamics (MD) Simulations

To study the distribution of ions (ammonium sulfate, AS) and organic molecules (3-methylglutaric acid, 3-MGA) within the droplet, we used OpenMM v7.3 (Eastman et al., 2017) to perform all-atom MD simulations of aqueous droplets containing AS and 3-MGA with an OIR of 1. This section consists of three parts:

(1) **Force Field Adjustment for the Systems**
(2) **Density Profiles**.
(3) **Simulation Details**

Before studying the density profiles (distributions) of the molecules/ions, we will first address the sticking problem between NH_4^+ and SO_4^{2-} typically found in classical MD simulations by modifying the interactions between N (in NH_4^+) and O (in SO_4^{2-}). Then, we will investigate the density profiles using our improved interaction parameters.

(1) Force Field Adjustment for the Systems

In our MD simulations, the forcefield for water was SWM4-NDP (Lamoureux et al., 2006), which is a polarizable water model. For the ions and 3-MGA, their parameters were obtained in GAAMP (Huang et al., 2013)

It is not uncommon to find sticking problems between anions and cations in classical MD simulations. For example, as shown in **Figure S7a**, the NH_4^+ (red) and SO_4^{2-} (blue) were attracted to each other too strongly and did not dissolve (mass ratio of AS to water was 0.048 in this example) in water. A common way to resolve the sticking problem is to adjust the Lennard-Jones (LJ) parameters between the ion pair to increase the repulsion between them while keeping the other interaction parameters unchanged, as shown in **Figure S7b**. We call this set of LJ parameters here the "original LJ parameters". Following the work of Luo and Roux (2010) and Yoo and Aksimentiev (2016), we modified the R_{min} in LJ between the N atoms in NH_4^+ and O atoms in SO_4^{2-} to match the experimental osmotic pressure of AS solution better (Robinson and Stokes, 1959).

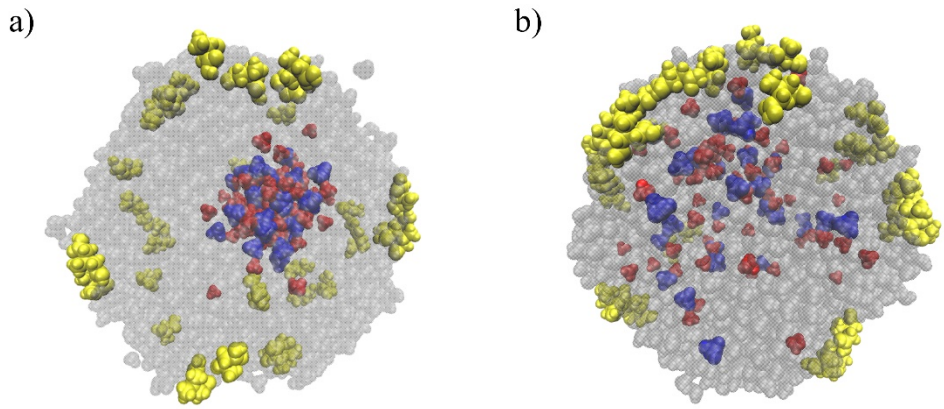

Figure S7. Simulation snapshot of a typical configuration of an aqueous droplet containing 5000 H_2O (gray), 30 3-MGA (yellow), 33 SO_4^{2-} (blue), and 66 NH_4^+ (red) at 300 K using a) the standard LJ parameters and b) corrected LJ parameters.

The results of osmotic pressure calculated with and without our LJ correction are compared with the experiment in **Figure S8**. We can see the calculated osmotic pressures with our correction can match the experimental curve better than that using the standard LJ parameters. The corrected LJ parameters are used in the following density profile calculations.

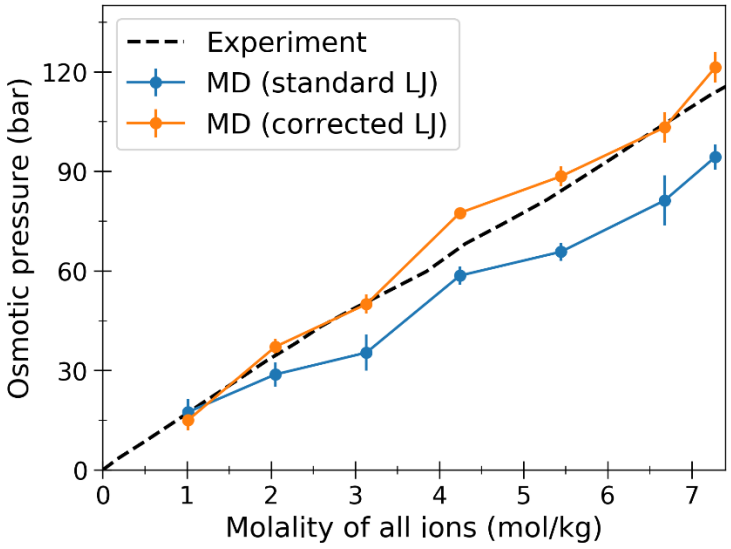

Figure S8. Osmotic pressure of AS solution as a function of solution molality calculated with standard LJ parameters (blue), corrected LJ parameters (orange), and experiment (black dashed line).

(2) Density Profiles

To investigate the distribution of the species within an aqueous droplet containing AS and 3-MGA with OIR = 1 at different values of relative humidity (RH), we calculated the density profiles for NH_4^+, SO_4^{2-}, and 3-MGA in aqueous droplets with different numbers of water molecules for both droplet and slab geometries as summarized in **Table S3**. For the slab geometry, the systems were fully periodic in the *xyz* directions. For the droplet setups, please see *Simulation Details*.

Table S3. Summary of MD simulation setups for droplets and slabs. Each setup has 30 3-MGA molecules, 33 SO_4^{2-}, and 66 NH_4^+ (OIR = 1).

Setup	Geometry	Number of H_2O	Mass fractions (%) 3-MGA/AS/H_2O
D1	droplet	1000	16.38/16.29/67.32
D2	droplet	3000	6.98/6.94/86.07
D3	droplet	5000	4.44/4.41/91.15
S1	slab	1000	16.38/16.29/67.32
S2	slab	3000	6.98/6.94/86.07
S3	slab	5000	4.44/4.41/91.15

For equilibration in each setup, the system was slowly heated up to 1000 K at a rate of 1 K/ps and was kept at 1000 K for at least 2 ns (no chemical changes are possible in this type of classical MD simulations). Then 5 independent configurations were collected from the last 100 ps trajectory and used to slowly cool down to 300 K at a rate of –1 K/ps and was kept at 300 K for at 10 ns before collecting at least 10 ns of production data, which was used to calculate the density profiles. Production simulation snapshots of each setup are shown in **Figure S9** for the droplets and in **Figure S10** for the slabs.

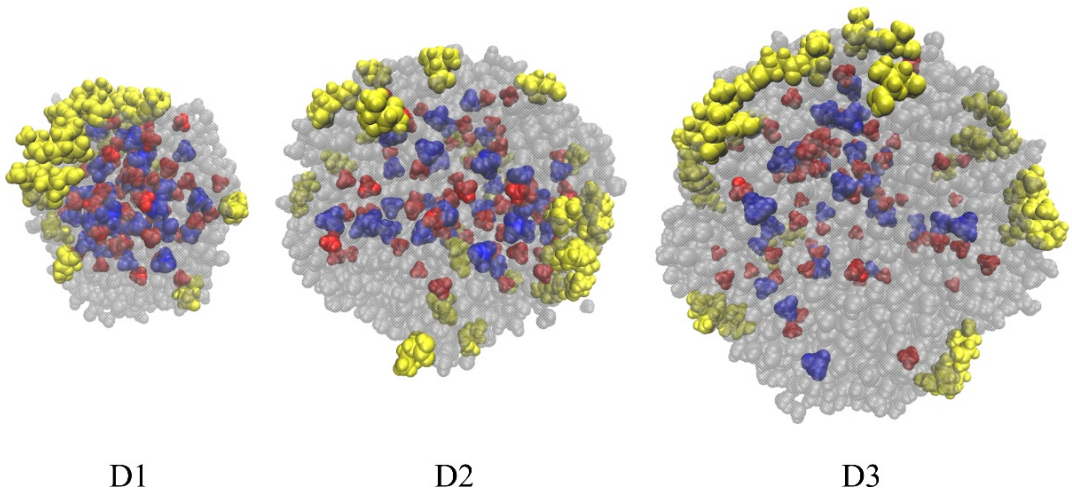

Figure S9. Simulation snapshots of typical configurations for droplet setups D1, D2, and D3. Same color scheme as in **Figure S7**.

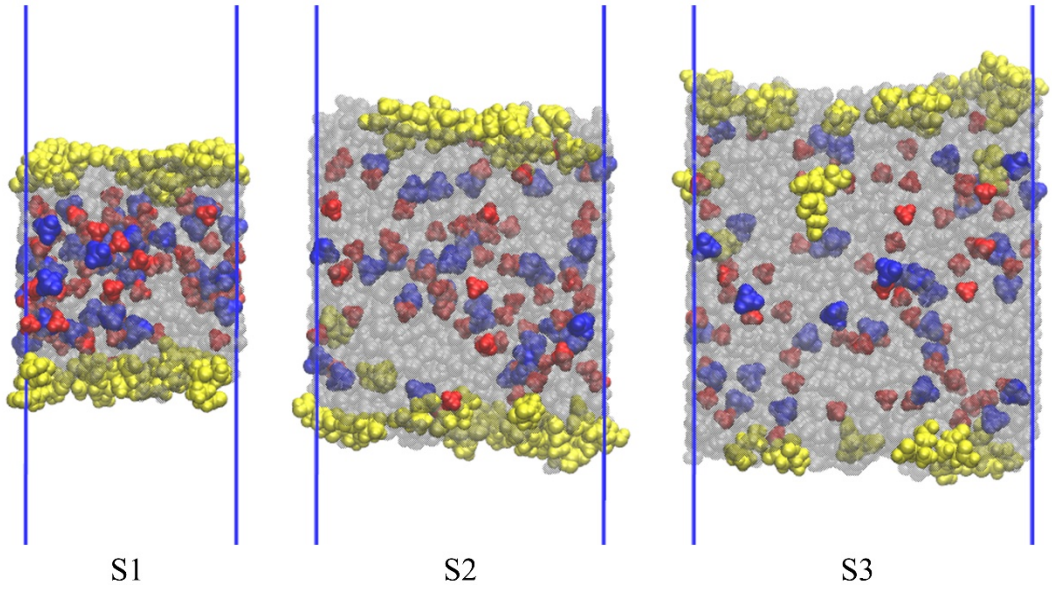

Figure S10. Simulation snapshots of typical configurations for slab setups S1, S2, and S3. Same color scheme as in **Figure S7**.

As shown in the simulation snapshots, 3-MGA (yellow) molecules tend to stay near the surface while the NH_4^+ (red) and SO_4^{2-} (blue) ions prefer to stay in the bulk, especially when the number of water molecules is small (D1 and S1). As the number of water molecules increases, a few 3-MGA molecules could diffuse into the bulk, but the majority remains near the surface. The density profiles for the setups shown in **Figures S11 and S12**.

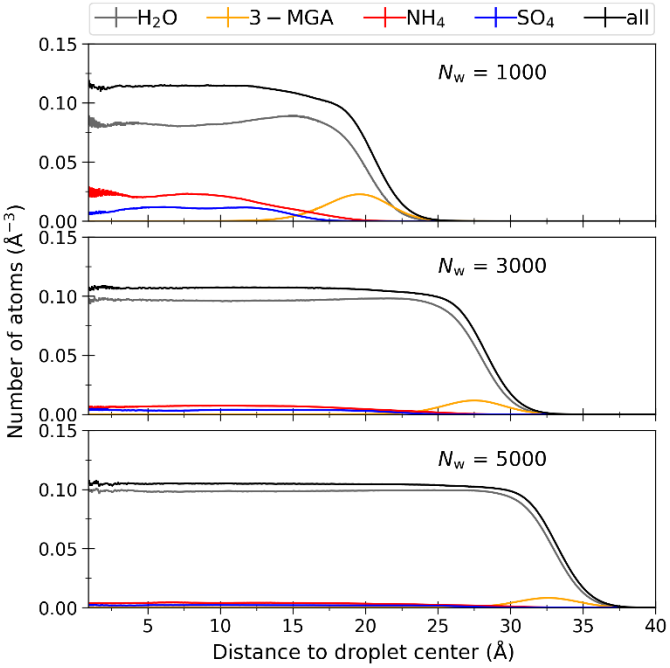

Figure S11. Number density profiles of H_2O, 3-MGA, NH_4^+, SO_4^{2-}, and their sum for the droplet setups D1 (top), D2 (middle), and D3 (bottom).

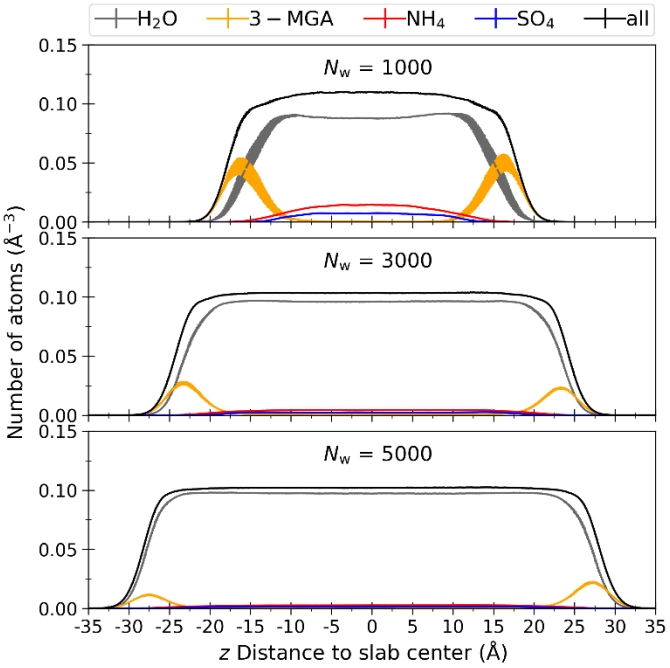

Figure S12. Number density profiles of H_2O, 3-MGA, NH_4^+, SO_4^{2-}, and their sum for the slab setups S1 (top), S2 (middle), and S3 (bottom).

(3) Simulation Details

Calculations of Osmotic Pressure in MD

To calculate the osmotic pressure of AS solution, we performed MD simulations of AS solutions at different AS concentrations. There were 7400 water molecules in each simulation and the AS concentration varied by having different numbers of NH_4^+ and SO_4^{2-} ions in the simulation box. In each simulation, two virtual semipermeable membranes parallel to the *yz* plane were applied to confine the NH_4^+ and SO_4^{2-} ions inside a cubic region of 50 × 50 × 50 Å (Huang et al., 2013), while water can pass through the semipermeable membranes freely. The whole setups were under periodic boundary conditions as shown in **Figure S13**. The semipermeable membranes were simulated by two half-harmonic potentials acting only on the ions:

$$V_{\text{semi}}(x) = \begin{cases} \frac{k}{2}\left(x - x_{\text{up}}\right)^2 & \text{for } x > x_{\text{up}} \\ 0 & \text{for } x_{\text{low}} \le x \le x_{\text{up}} \\ \frac{k}{2}\left(x - x_{\text{low}}\right)^2 & \text{for } x < x_{\text{low}} \end{cases} \quad \text{(S1)}$$

where k = 10 kcal mol^{-1}Å^{-2}, x, x_{up}, and x_{low} are the x coordinates of the ion, upper, and lower semipermeable membranes, respectively. Osmotic pressure can be estimated from the mean force per unit area exerted on the semipermeable membranes by the ions. The electrostatic interactions were calculated using PME (Essmann et al., 1995) with a cutoff of 14 Å for the real space. The LJ potential was switched to zero from 12 to 14 Å. The x dimension of the simulation box was initially set to 90 Å then relaxed under 1 bar pressure for 500 ps. The system was further equilibrated for 2 ns under constant *NVT* (number of atoms, volume, and temperature) at 298 K before production runs. The osmotic pressure of each setup was estimated by 5 independent 1.5 ns production runs. A time step of 1 fs was used for all the MD simulations.

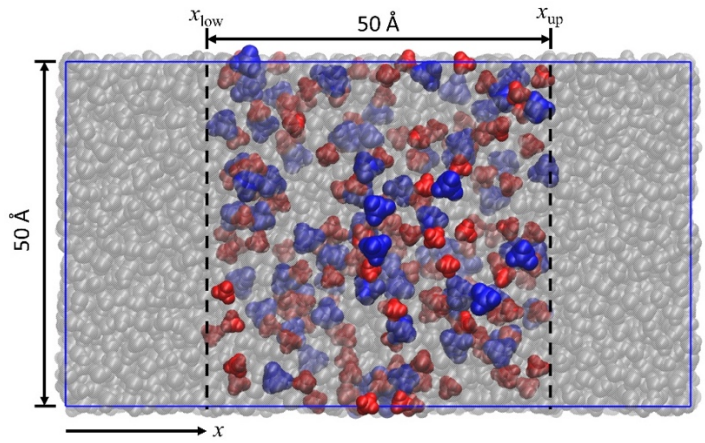

Figure S13. Simulation snapshot of an AS solution with two semipermeable membranes (indicated by the dashed lines). Same color scheme as in **Figure S7**. The molality of the ionic solution in the confined region is about 3.1 m in this example.

The original and corrected LJ parameters for the ion pair are shown in **Table S4**.

Table S4. Original LJ parameters and our correction.

	$\frac{1}{2}R_{\min}$ (Å)	Standard (Å)	corrected (Å)
N (in NH_4^+)	1.9755		
O (in SO_4^{2-})	1.6612		
N-O		3.6367	3.6658

Droplet setups

For each droplet setup, a flat-bottomed restraining potential was applied to prevent the atoms from leaving the simulation box:

$$V_d(r) = k_{wall}(r-R)^2 H(r-R) \quad \text{(S2)}$$

where k_{wall} = 0.1 kcal mol^{-1}Å^{-2} is the force constant, r is the radial distance of the atom from the droplet center, $H()$ is the Heaviside step function, R was set to ~5 Å larger than the droplet radius before cooling down and set to 60 Å after cooling down. Similarly, a flat-bottomed restraining potential in only the z direction was also applied to the slab setups before the system was cooled down:

$$V_s(z^*) = k_{wall}\left(|z^*| - \frac{D}{2}\right)^2 H\left(|z^*| - \frac{D}{2}\right) \quad \text{(S3)}$$

where z^* is the z distance of the atom from the slab center, D was set to ~10 Å larger than the slab thickness. All the intermolecular interactions were calculated explicitly without any cutoffs in the droplet setups while the cutoff scheme in the slab setups was the same as in the osmotic pressure simulations. The z dimension of the simulation box for the slab setups was all set to 150 Å, and the xy dimensions were set to 33 × 33 Å^2, 45 × 45 Å^2, and 53 × 53 Å^2 for S1, S2, and S3, respectively. The simulations were carried out at 298 K with a time step of 1 fs.

References

Eastman, P., Swails, J., Chodera, J. D., McGibbon R. T., Zhao, Y., Beauchamp, K. A., Wang, L.-P., Simmonett, A.C., Harrigan, M. P., Stern, C. D., Wiewiora, R. P., Brooks, B. R., and Pande, V. S.: OpenMM 7: Rapid development of high performance algorithms for molecular dynamics, PLOS Comput. Biol., 13, e1005659, https://doi.org/10.1371/journal.pcbi.1005659, 2017.

Essmann, U., Perera, L., Berkowitz, M. L., Darden, T., Lee, H., and Pedersen, L. G.: A smooth particle mesh ewald method, J. Chem. Phys., 103, 8577–8593, 1995.

Gržinić, G., Bartels-Rausch, T., Berkemeier, T., Türler, A., and Ammann, M.: Viscosity controls humidity dependence of N_2O_5 uptake to citric acid aerosol, Atmos. Chem. Phys., 15, 13615–13625, 2015.

Huang, L. and Roux B.: Automated force field parameterization for nonpolarizable and polarizable atomic models based on Ab Initio Target Data, J. Chem. Theory Comput., 9, 3543–3556, 2013.

Lamoureux, G., Harder, E., Vorobyov, I. V., Roux, B., and MacKerell, A. D. A.: Polarizable model of water for molecular dynamics simulations of biomolecules, Chem.

Phys. Lett., 418, 245–249, 2006.

Luo, Y. and Roux, B.: Simulation of Osmotic Pressure in Concentrated Aqueous Salt Solutions, J. Phys. Chem. Lett., 1, 183–189, 2010.

Robinson, R. A. and Stokes, R. H.: Electrolyte Solutions, Butterworths, 1959.

Yoo, J. and Aksimentiev, A.: Improved parameterization of amine–carboxylate and amine–phosphate interactions for molecular dynamics simulations using the CHARMM and AMBER force fields, J. Chem. Theory Comput., 12, 430–443, 2016